DOI: 10.1002/cmdc.200700113

Crystal Structure of the Bacterial Ribosomal Decoding Site Complexed with a Synthetic Doubly Functionalized Paromomycin Derivative: a New Specific Binding Mode to an A-Minor Motif Enhances in vitro Antibacterial Activity

Jiro Kondo,[b] Kandasamy Pachamuthu,[a] Boris François,[b] Janek Szychowski,[a] Stephen Hanessian,*[a] and Eric Westhof*[b]

*The crystal structure of the complex between oligonucleotide containing the bacterial ribosomal decoding site (A site) and the synthetic paromomycin analogue **1**, which contains the γ-amino-α-hydroxybutyryl (L-haba) group at position N1 of ring II (2-DOS ring), and an ether chain with an O-phenethylaminoethyl group at position C2′′ of ring III, is reported. Interestingly, next to the paromomycin analogue **1** specifically bound to the A site, a second molecule of **1** with a different conformation is observed at the crystal packing interface which mimics the A-minor interaction between two bulged-out adenines from the A site and the codon–anticodon stem of the mRNA–tRNA complex. Improved antibacterial activity supports the conclusion that analogue **1** might affect protein synthesis on the ribosome in two different ways: 1) specific binding to the A site forces maintenance of the "on" state with two bulged out adenines, and 2) a new binding mode of **1** to an A-minor motif which stabilizes complex formation between the ribosome and the mRNA–tRNA complex regardless of whether the codon–anticodon stem is of the cognate or near-cognate type.*

Introduction

Aminoglycosides are clinically important antibiotics targeting the bacterial ribosomal decoding site (A site) in the 30S ribosome.[1] The molecular mechanisms of their action on protein biosynthesis have been well investigated during the past decade.[2] It has been revealed by X-ray analyses that several types of natural aminoglycosides such as 4,5-disubstituted (for example, paromomycin and neomycin), 4,6-disubstituted (for example, geneticin and tobramycin), and 4-monosubstituted (for example, apramycin) aminoglycosides specifically bind to and stabilize the decoding "on" state of the A site in a conserved manner.[3–8] In other words, the A site, which is a molecular switch monitoring correct Watson–Crick base pairings between the mRNA codon and the tRNA anticodon, is always turned "on" in the presence of aminoglycosides, which eventually induces misreading of codons.[9–12]

Although they have been known as potent antibacterial agents, their widespread use in clinical practice has been compromised because of the rapid emergence of drug-resistant strains of bacteria.[1,13–15] Resistance to aminoglycosides arises mainly from 1) chemical modification of aminoglycosides by resistance enzymes and 2) chemical modification and/or point mutations of A-site nucleotides. To overcome this problem, modified aminoglycosides that can delay or avoid acquired resistance by pathogenic bacteria are required.

In preceding papers,[16–18] we reported several promising results of our analogue design paradigm by taking advantage of the structural information available from X-ray analyses. In the course of these studies, we have discovered a compound with potent antibacterial activity in both Gram-negative and Gram-positive bacteria. Compound **1** is a paromomycin derivative with a γ-amino-α-hydroxybutyryl (L-haba) group at position N1 of ring II, and a phenethylaminoethyl ether substituent group at position C2′′ of ring III. The former modification was first identified in the natural compound butirosin which may sterically disturb resistance enzyme recognition.[19] In addition, it has been revealed by X-ray analysis of the bacterial A site in complex with amikacin that the L-haba group can increase binding affinity of aminoglycosides to the A site through three

[a] *Dr. K. Pachamuthu, J. Szychowski, Prof. S. Hanessian*
Department of Chemistry, Université de Montréal
P.O. Box 6128, Station Centre-ville Montreal, P.Q., H3C3J7 (Canada)
Fax: (+1) 514-343-5728
E-mail: stephen.hanessian@umontreal.ca

[b] *Dr. J. Kondo, Dr. B. François, Prof. E. Westhof*
Architecture et Réactivité de l'ARN, Université Louis Pasteur
Institut de Biologie Moléculaire et Cellulaire, CNRS
15 rue René Descartes, 67084 Strasbourg (France)
Fax: (+33) 3-88-60-18-22
E-mail: E.Westhof@ibmc.u-strasbg.fr

additional direct contacts.[20] Introduction of a hydrophobic ether group at C2″ of paromomycin has resulted in the discovery of excellent first-generation lead compounds for the development of new and potent bactericidal aminoglycoside analogues.[16–18] Herein, we discuss the detailed structure of the bacterial A site complexed with the new synthetic paromomycin analogue **1**, revealing for the first time two types of specific binding modes. First the classical binding of **1** to the A site as observed for the C2″ ether analogues,[16,17] and second, a "new specific" binding to the A-minor motif exhibited by a second molecule of the same analogue **1**.

Results and Discussion

Overall structures

The 2D structure of crystallized RNA fragment and the 3D structure of the RNA–**1** complex are shown in Figures 1a and 2a, respectively. The overall conformation of the RNA duplex is almost identical with those previously reported for RNA–aminoglycoside complexes.[3–6,16,20] The root-mean-square deviations (RMSDs) of the corresponding atoms of RNA duplexes between the RNA–paromomycin complex[3] and the present RNA–**1** complex optimally superimposed are 1.1 Å. Four contiguous Watson–Crick G═C base pairs are formed at the center of duplex, and three Watson–Crick G═C base pairs close the stem at both ends. Overhanging cytosine residues are disordered in the solvent channel. A single aminoglycoside molecule specifically binds to the deep/major groove of each A site as regularly observed.[3–6,16,20] In addition, besides the analogue **1** inserted into the A site, a second molecule of **1** is present at the crystal packing interface (see Figure 2b).

Specific binding of 1 to the bacterial A site

Compound **1** is a 4,5-disubstituted aminoglycoside in the paromomycin series containing the L-haba group at position N1 of ring II and the phenethylaminoethyl ether chain at position C2″ of the ring III (see Figures 1b and 3a). As observed in previous papers,[6] key characteristic and common interactions between aminoglycosides and the bacterial A site, which help to stabilize the "on" state of the bacterial A site with bulged-out A1492 and A1493, are also conserved in the RNA–**1** complex. Thus, 1) ring I is inserted into the A site helix by stacking on the G1491 residue; 2) ring I forms a pseudo pair with the Watson–Crick sites of the universally conserved A1408 residue; and 3) ring II (2-DOS) makes four hydrogen bonds through N1–H···O4(U1495), N3–H···N7(G1494), N3–H···O2P(G1494), and N3–H···O1P(A1493).

The overall conformation and binding mode of **1** are very close to those of another paromomycin analogue **2** (PDB-ID: 2BE0) reported previously (see Figure 1b and 4a).[16] As observed in the RNA–**2** complex, rings III and IV of **1** are also oriented very differently from the parent paromomycin in the A site.[3] There is a 40° flip around the β-D-ribofuranosyl linkage of the paromamine unit compared to paromomycin. The sugar pucker of ring III also changes from C2′-*endo* in paromomycin to C3′-*endo* in **1**. As a result, the orientation of ring IV in **1** rotates 90° from that observed in paromomycin. All 12 direct contacts between the paromomycin moiety and the A site observed in the RNA–**2** complex are conserved in the RNA–**1** complex (the H-bond O6-H···O4(U1406) is observed in only one A site with symmetrical U1406oU1495 base pair, see Figure 3i). In addition to the direct

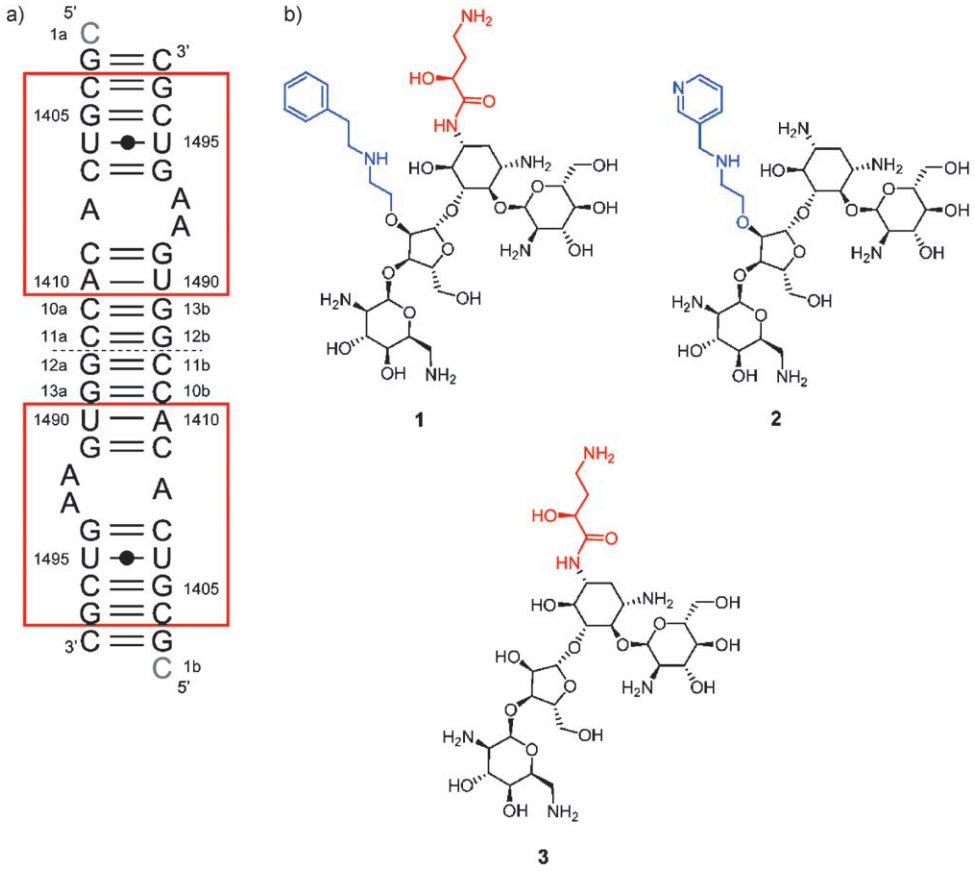

Figure 1. a) Secondary structure of the crystallized RNA duplex. The two bacterial A sites are boxed and the unobserved 5′-overhanging cytosine residues are gray. Geometric nomenclature and classification of nucleic acid base pairs are according to the classification in reference [30]. b) Chemical structures of paromomycin analogues **1**, **2**, and **3**. The paromomycin moiety, the L-haba group, and the ether chain at C2″ of ring III with the phenethylaminoethyl group are colored black, red, and blue, respectively.

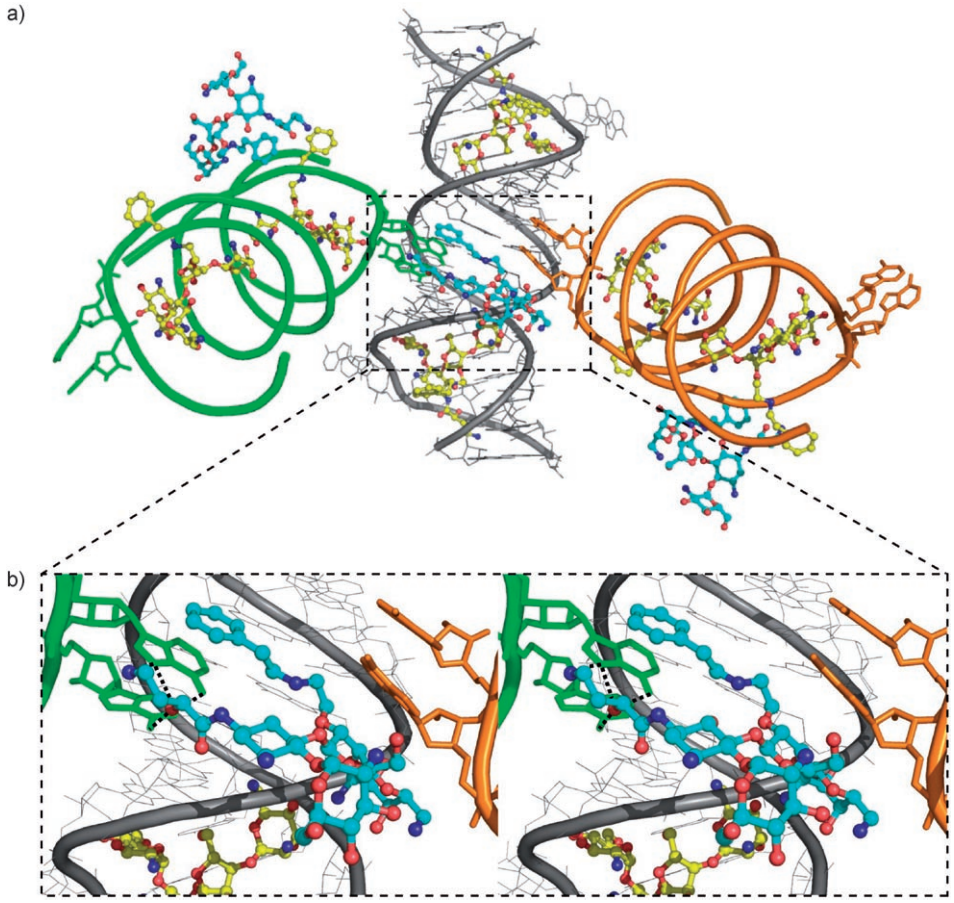

Figure 2. Three-dimensional structure of the crystal packing interaction in a) the RNA–**1** crystal and b) its local stereoview. The view in a) shows a central duplex (gray) interacting with two symmetry-related duplexes (green and orange) through the A-minor motif with two bulged-out adenines, A1492 and A1493 (orange and green). The specifically (yellow) and "new specifically" (cyan) bound **1**, shown in ball and stick, recognize the A site and the A-minor motif respectively.

contacts, nine water-mediated contacts are observed between **1** and the A site atoms. The hydrophobic ether chain at position C2″ extends across the deep/major group of the A site, points into the solvent, and forms no direct contact with the RNA (see Figure 3a).

The stereoview of the specific interaction of the L-haba group in **1** to the bacterial A site is shown in Figure 5. As observed in the previously reported RNA–amikacin (PDB-ID: 2G5Q) and two RNA–neamine-derivative complexes (PDB-ID: 2F4T and 2F4U),[19,21] the L-haba group interacts with the upper side of the A site (see Figures 4b and 5). Three direct contacts, O2*–H···N4(C1496), O2*–H···O4(U1495), and N4*–H···O6(G1497), and one water-mediated contact, O2*–H···W···O2P(U1495), are observed in the RNA–**1** complex (a direct contact N4*–H···N4-(C22b) and a water-mediated contact N4*–H···W···O6(G2a) are also observed, but the C22b and G2a residues are outside the usual span of the A site). One of two direct contacts, N4*–H···O6(G1497), is not observed in the two RNA–neamine-derivative complexes (solved at 2.6 and 3.0 Å), because the N4* atom of the L-haba group points away from the G1497 residue (see Figure 4b). The O1* atom of the L-haba group is not involved in any interaction with the A site. It is important to note that, although amikacin and the two neamine-derivatives are 4,6-disubstituted aminoglycosides, the interaction patterns between the A site and the L-haba group in **1** are practically conserved.

A new binding of 1 to the A-minor motif

Besides the specifically bound **1** in the A site, a second molecule of **1** is present at the crystal packing interface (see Figure 2b). Its conformation is almost identical to the commonly observed pattern in paromomycin, and different from that of **1** specifically bound to the A site (see Figure 6a). As in the case of paromomycin, ring III of **1** in the second bound molecule adopts the usual C2′-*endo* sugar pucker, whereas in the A site bound molecule **1** it is C3′-*endo*. The phenethylaminoethyl chain at position C2″ is stabilized by an intramolecular hydrogen bond O6–H···N3**. The second bound molecule **1** with the new conformation makes four direct contacts with the bulged-out A1492 and A1493 by using the L-haba group and two direct contacts with the G=C stem of a neighboring RNA duplex in conjunction with ring IV (see Figure 6a–c). In addition to these hydrogen-bonding contacts, the *O*-phenethylaminoethyl group stacks on the A1492 residue (see Figure 6c–e). As a result, the bound **1** in the new conformation stabilizes the A-minor motif between the two bulged-out adenines and the central G=C base pairs, belonging to a symmetrically-related molecule and that mimic the codon–anticodon stem.

This additional binding mode for analogue **1** is completely different from the nonspecific binding modes found around the A site in the RNA–kanamycin, RNA–ribostamycin, RNA–neomycin, and RNA–neomycin-derivative complexes.[6,8] In the first complex, one of the two A sites contains two bound kanamycin molecules, one in the specific binding mode and the other one in the nonspecific binding mode. In the second complex, both A sites contain two bound ribostamycin molecules, one in the specific binding mode and the other one still in the nonspecific binding mode. And, in the third and fourth complexes, besides specifically bound neomycin or neomycin-derivative molecule in the A site, one nonspecifically bound aminoglycoside is present in the deep/major groove at the interface of coaxially stacked RNA helices. All these nonspecifically bound

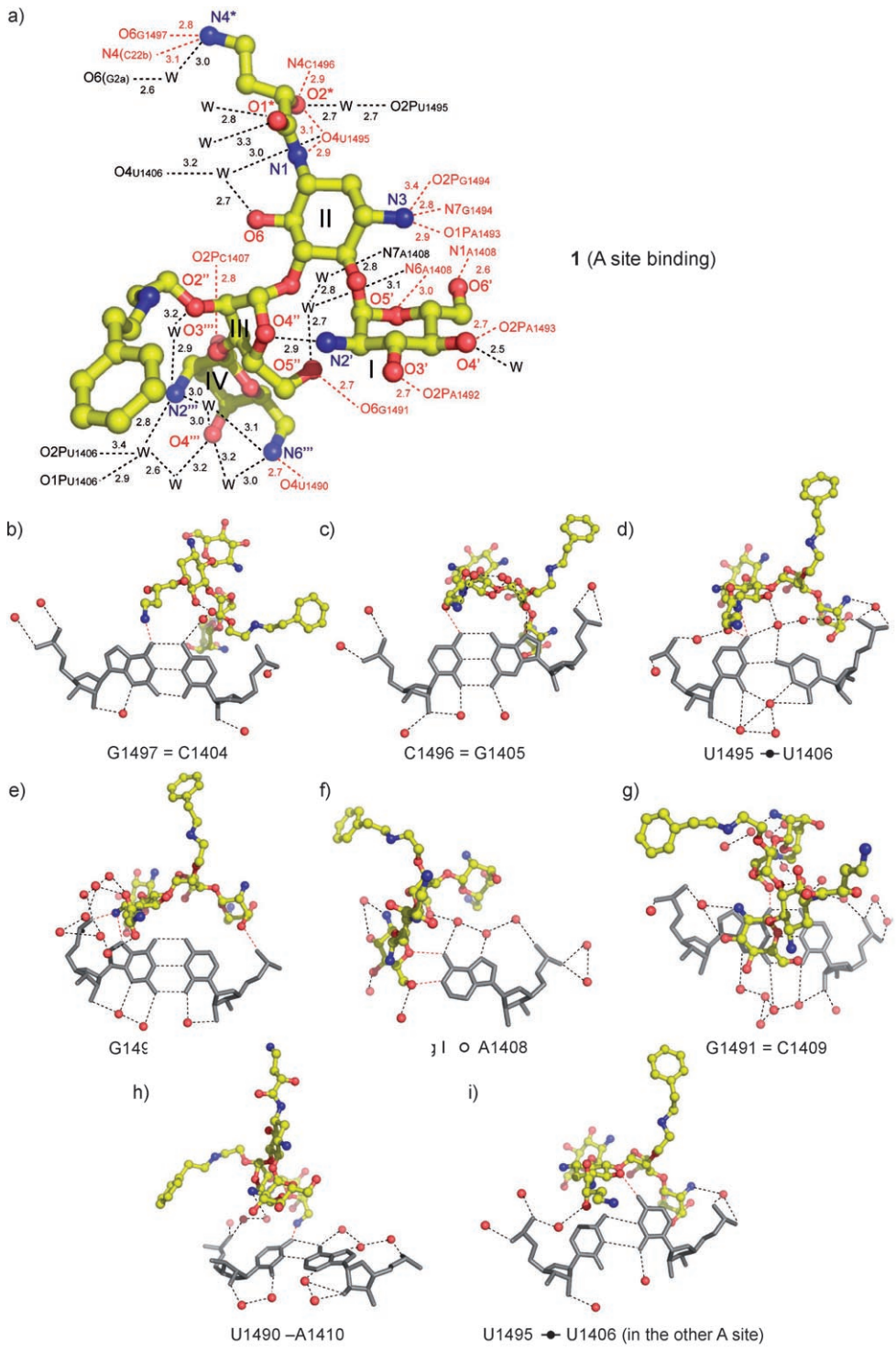

Figure 3. Specific binding of **1** to the bacterial A site. a) Structure adopted by compound **1** inside the bacterial A site. Ring number (I–IV) and atom names are specified. The *E. coli* numbering is used for the RNA atoms, and 'W' stands for water molecule. b–i) Atomic details of the contacts involving each base pair of the minimal A site interacting with **1**. Direct contacts and water-mediated contacts between **1** and the minimal A site are shown in red and black dashed lines, respectively.

aminoglycosides do not play any key role, neither forcing two adenine residues to be bulged out, nor stabilizing the A-minor contacts between these two adenines and the Watson–Crick pairs. In contrast, in the present complex, the second molecule **1** makes specific contacts and stabilizes the A-minor motif. Therefore, we refer to this new binding mode found in the present RNA–**1** complex as the "new specific" binding mode.

An important question is whether the "new specific" binding mode of **1** to the A-minor motif has any beneficial effect in its antibacterial activity. To answer this question, we have determined the minimal inhibitory concentration (MIC) of **1** in wild type Gram-negative (*Escherichia coli*) and Gram-positive (*Staphylococcus aureus*) bacteria, and have compared them with those of the parent paromomycin and two paromomycin derivatives with only a single modification, that is addition of the L-haba group at position N1 of ring II (compound **3**), or the ether chain with the 2-*N*-(3-pyridylmethyl)-ethylamino group at position C2′′ of ring III (compound **2**) (see Table 2 and Figure 1 b).[18,19] Surprisingly, addition of the L-haba group at position N1 of paromomycin does not improve antibacterial activity, although the L-haba group can interact with the upper side of the A site with three direct and one water-mediated contact as discussed above (indeed compound **3** has higher binding affinity to a prototypical segment of the 16S bacterial A site than paromomycin[22]). Addition of the hydrophobic ether chain at position C2′′ of paromomycin as in compound **2** slightly improves antibacterial activity only in *S. aureus* but not in *E. coli*. On the other hand, compound **1** with the double modification has a superior level of antibacterial activity compared to parent paromomycin in both *E. coli* and *S. aureus*, though compound **1** has a similar K_D compared to compounds **2** and **3**. These results indicate that the improvement of antibacterial activity with the dual modification might be related to the binding of the aminoglycoside in the "new specific" mode to the A-minor motif between two bulged-out adenines from the A site and the codon–anticodon stem of the mRNA–tRNA complex.

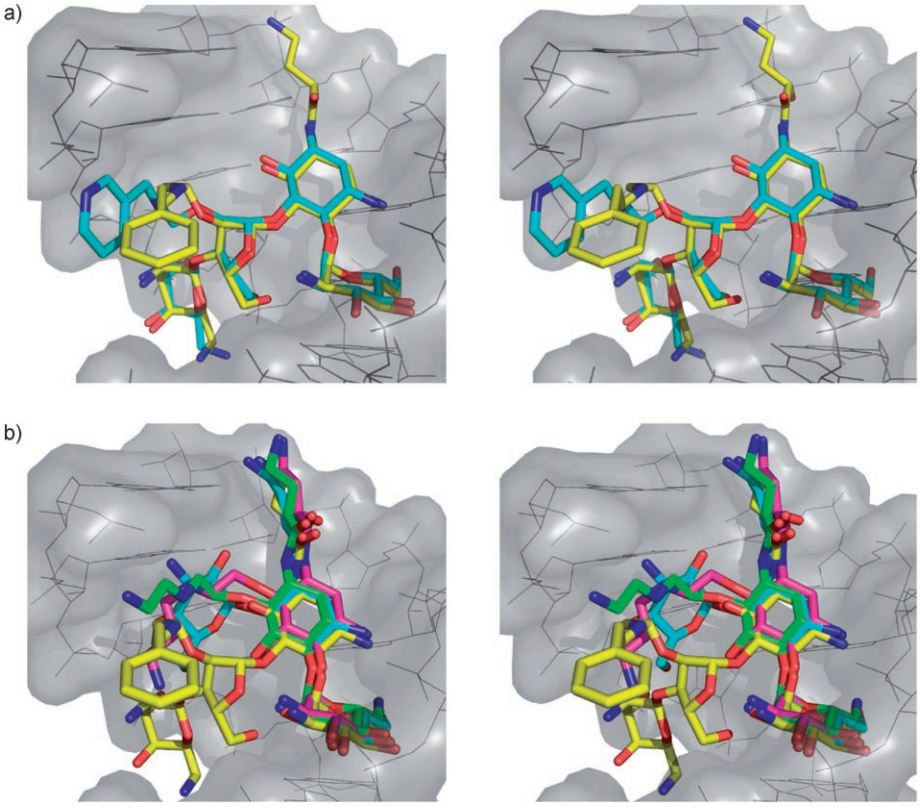

Figure 4. Stereoviews of superimposition between a) **1** (yellow) and **2** (cyan, PDB-ID: 2BE0), and b) between **1** (yellow), amikacin (cyan, PDB-ID: 2G5Q), neamine-derivative 1 (green, PDB-ID: 2F4T), and neamine derivative 2 (pink, PDB-ID: 2F4U) in the bacterial A site helix.

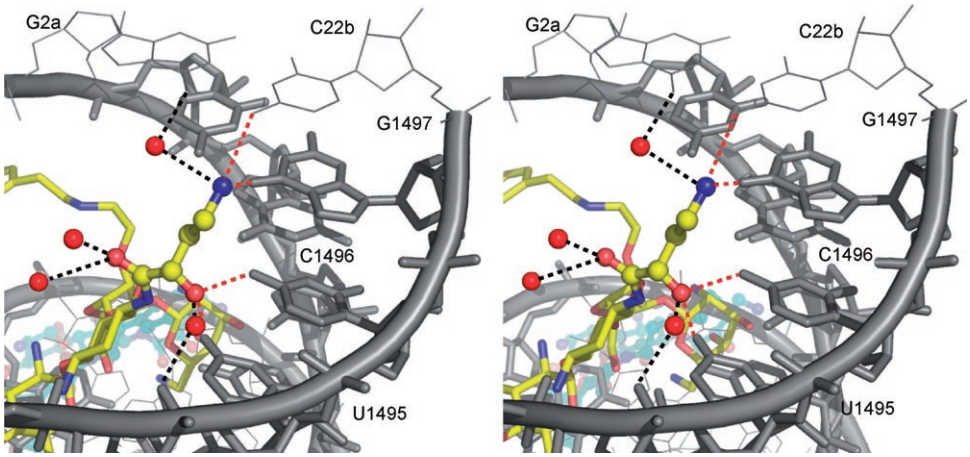

Figure 5. Stereoview of specific interactions of the L-haba group in **1** to the bacterial A sites. Direct contacts and water-mediated contacts are shown in red and black dashed lines, respectively.

Conclusion

The conclusions derived from the present work can be summarized as follows. 1) Compound **1** specifically binds to the A site like its parent paromomycin and other aminoglycoside antibiotics with the conformation of ring III different from that of the parent paromomycin but identical to that in the 2-*N*-(3-pyridylmethyl)-ethylamino ether analogue **2**; 2) The L-haba group in **1** interacts with the upper side of the A site as observed in the RNA–amikacin and two RNA–neamine-derivative complexes; 3) A "new specific" binding mode of **1** stabilizing the A-minor motif is observed with the conformation of ring III different from that in the "specific" bound molecule in the A site, suggesting that conformational switching allows **1** to select two different targets; 4) Results from antibacterial activity assays suggest that **1** might affect protein synthesis in two different ways: a) specific binding to the A site maintains the "on" state with two bulged-out adenines and b) the "new specific" binding to an A-minor motif which stabilizes complex formation between ribosomes and the mRNA–tRNA complex, eventually inducing misreading of the codon. Very recently, it has been confirmed that the cyclic peptide antibiotic viomycin binds the ribosome near the intersubunit bridge formed between 16S rRNA helix 44 and 23S rRNA helix 69, and stabilizes the intermediate state of ribosomal translocation.[23] By analogy with the binding mode of viomycin, the "new specific" binding of **1** to an intersubunit A-minor motif may induce similar effects on protein synthesis. A synergistic effect of these two specific binding modes could provide an explanation of the potent antibacterial activity of **1** in both wild type Gram-negative and Gram-positive bacteria exemplified by *E. coli* and *S. aureus*.

Past efforts toward the synthesis of aminoglycoside analogues targeting the 30S ribosome have been concerned with increasing their affinity to the A site.[24] The dual binding modes exhibited by analogue **1**, targeting the A site and the A-minor motif presents a new paradigm for aminoglycoside modification with the objective to overcome resistance and/or to point mutations of A-site nucleotides. Preliminary studies indicate that no O3′-phosphorylation was detectable for analogues **1** and **2** in the presence of APH(3′)-

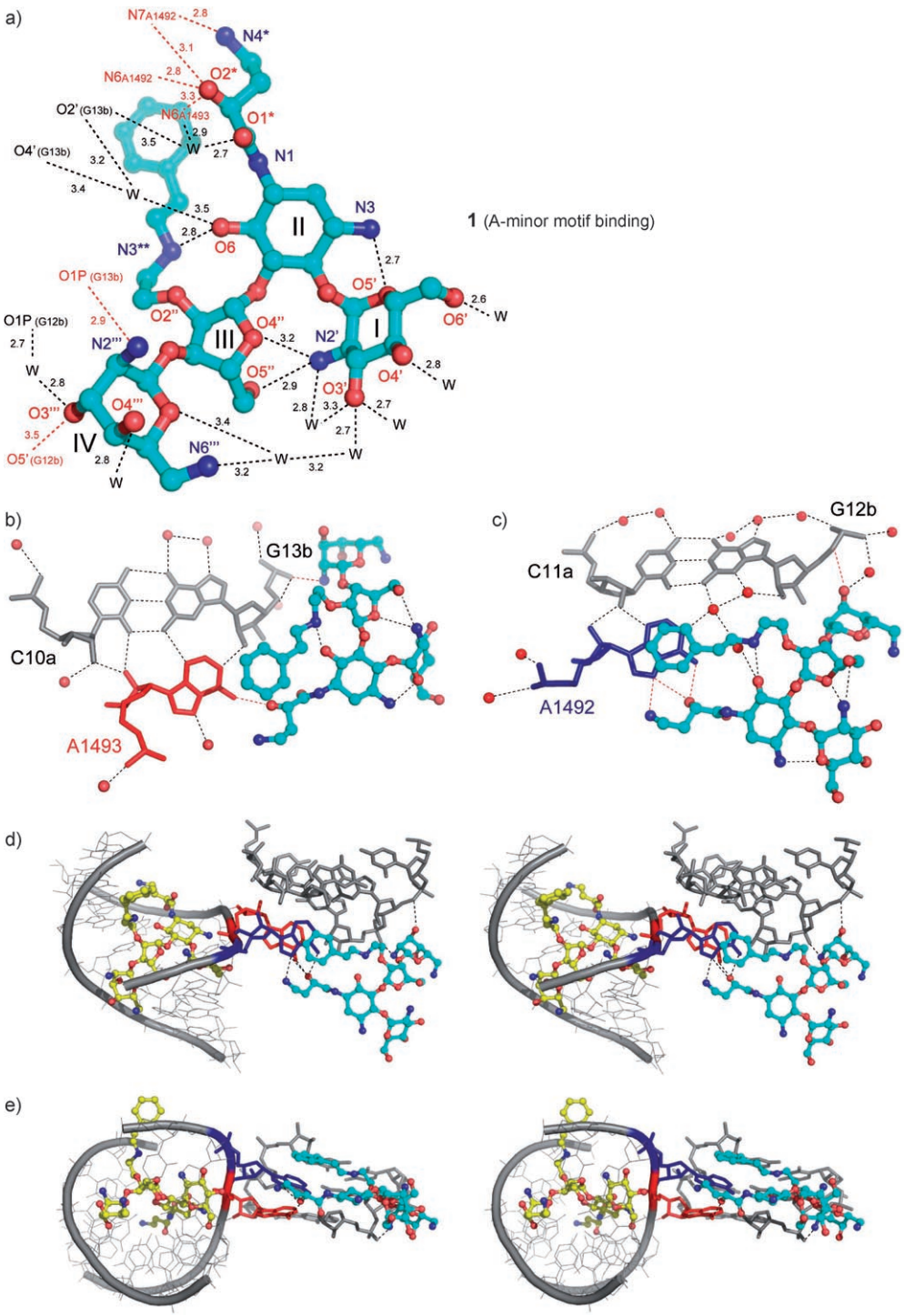

Figure 6. "New specific" binding of **1** to the A-minor motif. a) Contacts made by the "new specific" bound **1**. Ring number (I–IV) and atom names are specified. The numbering used for the RNA atoms corresponds to that in Figure 1a, and "W" stands for water molecule. b) and c) Atomic details of the contacts between **1** and RNA atoms. d) and e) Stereoviews of the intermolecular A-minor interaction stabilized with "new specific" binding of **1**. Direct contacts and water-mediated contacts between analogue **1** and RNA atoms are shown in red and black dashed lines, respectively.

IIIa.[25] Results pertaining to these and related aspects of aminoglycosides modifications will be communicated in due course.

Experimental Section

Crystallization

Crystallization procedures are essentially the same as published previously.[3–6,16,20] The asymmetrical loop of the bacterial A site was inserted between Watson–Crick pairs in sequences designed to fold as a double helix (see Figure 1a). The RNA oligomer was synthesized by Dharmacon (Boulder, CO) and purified by HPLC and reverse phase chromatography. Prior to crystallization, compound **1** (see Figure 1b) was dissolved at 4 mM in 50 mM sodium cacodylate buffer (pH 6.4), and 2 mM RNA solution containing 100 mM sodium cacodylate (pH 6.4), 25 mM sodium chloride and 5 mM magnesium sulfate was annealed by heating at 85 °C for 2 min followed by slow cooling to 37 °C. Same volumes of RNA solution and aminoglycoside solution were mixed at 37 °C and then cooled the mixture slowly to room temperature (21–25 °C).

Crystallization was performed by the hanging-drop vapor diffusion method at 37 °C as follows, 1 μL of RNA–**1** solution was combined with 1 μL of crystallization solution containing 1–5% (*v/v*) 2-methyl-2,4-pentanediol and 1–5% (*v/v*) glycerol, and equilibrated over a 50% (*v/v*) 2-methyl-2,4-pentanediol reservoir. Suitable crystals for X-ray experiments were recovered and vitrified in liquid ethane after soaking briefly in cryoprotectant containing 125 mM sodium cacodylate (pH 6.4), 12.5 mM sodium chloride, 150 mM potassium chloride, 2 mM **1**, and 40% 2-methyl-2,4-pentandiol.

Data collection, structure determination, and refinement

X-ray data were collected at 100 K with synchrotron radiation (0.9999 Å) at the PX beamline in the Swiss Light Source (SLS; Villingen, Switzerland) with a CCD detector (marCCD) set 200 mm from the crystal. Oscillations and exposure times were 1° and 1 s. Images were processed at a resolution of 1.8 Å with the program Crystalclear (Rigaku/MSC). The crystal belongs to the space group $P2_12_12_1$ with unit cell dimensions $a=35.5$ Å, $b=43.0$ Å, $c=98.8$ Å. R_{merge} and completeness are 7.0% and 100% for the 14605 unique reflections, respectively. The statistics of data collection and the crystal data are summarized in Table 1.

Table 1. Crystal data, statistics of data collection, and structure refinement for analogue **1**.

Crystal data	
Space group	$P2_12_12_1$
Unit cell [Å]	$a=35.5$, $b=43.0$, $c=98.8$
Z[a]	1
Data collection	
Beamline	PX of SLS
Wavelength [Å]	0.9999
Resolution [Å]	32.4–1.8
of the outer shell [Å]	1.9–1.8
Observed reflections	278 304
Unique reflections	14 605
Completeness [%]	100.0
in the outer shell [%]	100.0
R_{merge}[b] [%]	7.0
in the outer shell [%]	60.9
Redundancy	19.1
in the outer shell	11.2
Refinement	
Resolution range [Å]	32.0–1.8
Used reflections	14 603
R-factor[c] [%]	21.1
R_{free}[d]	24.3
Number of DNA atoms	900
Number of antibiotic molecules	3
Number of water molecules	206
RMSD	
Bond length [Å]	0.006
Bond angles [°]	0.9
Improper angles [°]	1.3

[a] Number of dsRNA in the asymmetric unit. [b] $R_{merge}=100\,\Sigma_{hklj}|I_{hklj}-<I_{hklj}>|/\Sigma_{hklj}<I_{hklj}>$. [c] R-factor $=100\,\Sigma||F_o|-|F_c||/\Sigma|F_o|$, where $|F_o|$ and $|F_c|$ are optimally scaled observed and calculated structure factor amplitudes, respectively. [d] Calculated using a random set containing 10% of observations that were not included throughout refinement.[29]

Table 2. Antibacterial activities of paromomycin derivatives.

Aminoglycoside	L-haba[a]	Side chain at C2″[b]	K_D [μM][c]	MIC [μM][d] *E. coli*	MIC [μM][d] *S. aureus*
Paromomycin	No	No	0.15	2.5–5	1.2–2.5
1	Yes	Yes	0.1184	0.6–1.3	0.6–1.2
2	No	Yes	0.13	12–25	<1.5
3	Yes	No	0.0866	5.0–10	1.3–2.5

[a] Presence of the L-haba group at position N1 of paromomycin ring II. [b] Presence of the ether chain with *O*-phenethylaminoethyl group (compound **1**) or 2-*N*-(3-pyridylmethyl)-ethylamino group (compound **2**) at position C2″ of paromomycin ring III. [c] Dissociation constants with a prototypical segment of 16S bacterial A site. [d] Minimal inhibitory concentrations in Gram-negative (*Escherichia coli*) and Gram-positive bacteria (*Staphylococcus aureus*).

The RNA–**1** crystal is in the same spacegroup and has unit cell dimensions similar to the previously reported RNA–paromomycin crystal[3] suggesting isomorphism of the two crystals. Therefore the crystal structure of the RNA–paromomycin complex (PDB code: 1J7T) was used as a probe for the molecular replacement method. All MR calculations were performed with the program AMoRe.[26] The atomic parameters of the structure were refined with the program CNS[27] through a combination of rigid-body refinement, simulated-annealing, crystallographic conjugate gradient minimization refinements, and *B*-factor refinements, followed by interpretations of the omit map at every nucleotide residue. The parameters and topology files for molecule **1** was obtained on the Heterocompound Information Center-Uppsala server (University of Uppsala, Sweden).[28] The statistics of structure refinement are summarized in Table 1. Crystallized RNA duplex contains two identical but independent A sites, and one of the two A sites is better defined structurally (lower temperature factors and more identified solvent peaks). Therefore, in Figures 3 and 5, only the better defined A site is used to represent the specific binding interaction with compound **1**. Figures 2–6 were drawn using The PyMOL Molecular Graphics system (2002) DeLano Scientific, San Carlos, CA.[31]

Acknowledgements

During part of this work, Dr. J. Kondo was supported by Japan Society for the Promotion of Science. We thank the Swiss Light Source for provision of synchrotron radiation facilities and acknowledge the people of beamline PX in SLS.

Keywords: aminoglycoside · a-minor motif · L-haba group · ribosomal decoding site · X-ray analysis

[1] a) S. B. Vakulenko, S. Mobashery, *Clin. Microbiol. Rev.* **2003**, *16*, 430–450; b) S. Magnet, J. S. Blanchard, *Chem. Rev.* **2005**, *105*, 477–497.
[2] a) H. F. Noller, *Science* **2005**, *309*, 1508–1514; b) D. Moazed, H. F. Noller, *Nature* **1987**, *327*, 389–394.
[3] Q. Vicens, E. Westhof, *Structure* **2001**, *9*, 647–658.
[4] Q. Vicens, E. Westhof, *Chem. Biol.* **2002**, *9*, 747–755.
[5] Q. Vicens, E. Westhof, *J. Mol. Biol.* **2003**, *326*, 1175–1188.
[6] B. François, R. J. M. Russell, J. B. Murray, F. Aboul-ela, B. Masquida, Q. Vicens, E. Westhof, *Nucleic Acids Res.* **2005**, *33*, 5677–5690.
[7] Q. Han, Q. Zhao, S. Fish, K. B. Simonsen, D. Vourloumis, J. M. Froelich, D. Wall, T. Hermann, *Angew. Chem.* **2005**, *117*, 2754–2760; *Angew. Chem. Int. Ed.* **2005**, *44*, 2694–2700.
[8] F. Zhao, Q. Zhao, K. F. Blount, Q. Han, Y. Tor, T. Hermann, *Angew. Chem.* **2005**, *117*, 5463–5468; *Angew. Chem. Int. Ed.* **2005**, *44*, 5329–5334.
[9] J. M. Ogle, D. E. Brodersen, W. M. Clemons, Jr., M. J. Tarry, A. P. Carter, V. Ramakrishnan, *Science* **2001**, *292*, 897–902.
[10] J. M. Ogle, A. P. Carter, V. Ramakrishnan, *Trends Biochem. Sci.* **2003**, *28*, 259–266.
[11] J. M. Ogle, F. V. Murphy, M. J. Tarry, V. Ramakrishnan, *Cell* **2002**, *111*, 721–732.
[12] J. M. Ogle, V. Ramakrishnan, *Annu. Rev. Biochem.* **2005**, *74*, 129–177.
[13] M.-P. Mingeot-Leclercq, Y. Glupczynski, P. M. Tulkens, *Antimicrob. Agents Chemother.* **1999**, *43*, 727–737.
[14] J. Davies, G. D. Wright, *Trends Microbiol.* **1997**, *5*, 234–240.
[15] P. Pfister, S. Hobbie, Q. Vicens, E. C. Böttger, E. Westhof, *ChemBioChem* **2003**, *4*, 1078–1088.
[16] B. François, J. Szychowski, S. S. Adhikari, K. Pachamuthu, E. E. Swayze, R. H. Griffey, M. T. Migawa, E. Westhof, S. Hanessian, *Angew. Chem.* **2004**, *116*, 6903–6906; *Angew. Chem. Int. Ed.* **2004**, *43*, 6735–6738.
[17] S. Hanessian, J. Szychowski, S. S. Adhikari, G. Vasquez, P. Kandasamy, E. E. Swayze, M. T. Migawa, R. Ranken, B. François, J. Wirmer-Bartoschek, J. Kondo, E. Westhof, *J. Med. Chem.* **2007**, *50*, 2352–2369.
[18] S. Hanessian, J. Szychowski, S. S. Adhikari, K. Pachamuthu, M. T. Migawa, R. H. Griffey, WO 06/052930, 2006; [*Chem. Abstr.* **2006**, *144*, 468 397].
[19] R. J. M. Russell, J. B. Murray, G. Lentzen, J. Haddad, S. Mobashery, *J. Am. Chem. Soc.* **2003**, *125*, 3410–3411.
[20] J. Kondo, B. François, R. J. Russell, J. B. Murray, E. Westhof, *Biochimie* **2006**, *88*, 1027–1031.
[21] J. B. Murray, S. O. Meroueh, R. J. Russell, G. Lentzen, J. Haddad, S. Mobashery, *Chem. Biol.* **2006**, *13*, 129–138.
[22] S. Hanessian, M. Tremblay, E. E. Swayze, *Tetrahedron* **2003**, *59*, 983–993.
[23] D. N. Ermolenko, P. C. Spiegel, Z. K. Majumbar, R. P. Hickerson, R. M. Clegg, H. F. Noller, *Nat. Struct. Mol. Biol.* **2007**, *14*, 493–497.

[24] See for example: a) J. Lie, C-W. T. Chang, *Anti-Infect. Agents Med. Chem.* **2006**, *5*, 255 – 271; b) J. G. Silva, I. Carvalho, *Curr. Med. Chem.* **2007**, *14*, 1101 – 1119.
[25] J. W. Keillor, J. Szychowski, S. Hanessian, unpublished results.
[26] J. Navaza, *Acta Crystallogr. Sect. A* **1994**, *50*, 157 – 163.
[27] A. T. Brünger, P. D. Adams, G. M. Clore, W. L. DeLano, P. Gros, R. W. Grosse-Kunstleve, J-S. Jiang, J. Kuszewski, M. Nilges, N. S. Pannu, R. J. Read, L. M. Rice, T. Simonson G. L. Warren, *Acta Crystallogr. D* **1998**, *54*, 905 – 921.
[28] G. J. Kleywegt, T. A. Jones, *Acta Crystallogr. Sect. D* **1998**, *54*, 1119 – 1131.
[29] A. T. Brünger, *Nature* **1992**, *355*, 472 – 475.
[30] N. B. Leontis, E. Westhof, *RNA* **2001**, *7*, 499 – 512.
[31] http://www.pymol.org.

Received: May 15, 2007
Revised: July 21, 2007
Published online on August 27, 2007

